MODELING NEUTROPHIL DYNAMICS IN SEPSIS AND CANCER TREATMENT

Thang Ho, [*] **Gilles Clermont,** [**] **Robert S. Parker** [*,1]

[*] *Department of Chemical and Petroleum Engineering, University of Pittsburgh, Pittsburgh, PA*
[**] *Department of Critical Care Medicine, University of Pittsburgh Medical Center, Pittsburgh, PA*

Abstract: A mathematical model of neutrophil and granulocyte colony stimulating factor (G-CSF) dynamics is developed to capture the response of circulating neutrophil levels to inflammatory and anticancer drug challenges. Severe infection or trauma induces inflammation, leading to: (i) the recruitment of neutrophils to the site of infection; (ii) misdirected neutrophil recruitment to healthy tissue, which causes damage; and (iii) an increase in neutrophil production through the G-CSF signaling cascade. The limiting element of cancer chemotherapy is often toxicity. Some drugs kill neutrophil precursor cells, leading to a decrease in the absolute neutrophil count in blood. Starting from the 6 compartment model of Friberg *et al.* (2002), the model is extended to capture neutrophil and G-CSF dynamics in response to both inflammation and chemotherapy using lipopolysaccharide (inflammatory) and docetaxel (chemotherapy) response data. As a more complex inflammatory challenge, cecal ligation and puncture (CLP) is simulated, and the model is consistent with neutrophil and G-CSF data from the literature. The expanded biology in this model provides a superior structure for use in designing and evaluating treatments aimed at modulating neutrophil dynamics in severe infections.

Keywords: Nonlinear dynamic modeling, inflammation, sepsis, cancer chemotherapy, neutrophils, LPS, G-CSF.

1. INTRODUCTION

Sepsis is the systemic inflammatory response of the body to infection and is the second leading cause of death in the intensive care unit (ICU) (Angus and Wax, 2001). Treatment of sepsis has been a challenge for not only medical doctors but also scientists whose goals are to understand the dynamics of the physiological inflammatory response to sepsis, to identify the response of important markers during the disease progression (including pro- and anti-inflammatory cytokines), and ultimately to develop more effective and more successful treatment to inflammation and sepsis (Parker and Clermont, 2010; Rivers *et al.*, 2001; Mathe *et al.*, 2009).

Computational modeling efforts have been able to capture certain dynamics of the pro-inflammatory cytokines (*e.g.*, interleukin-1 (IL-1), IL-6, and tumor necrosis factor (TNF)) and anti-inflammatory cytokines (*e.g.*, IL-1 receptor antagonist (IL-1ra), IL-10, soluble TNF receptor 1 (TNFR1), and soluble TNFR2) (Rosinski *et al.*, 2004; Summers *et al.*, 2010). Significant collaborative effort between computational and experimental groups have improved understanding about inflammatory response and have begun to identify the important factors that dictate the outcome of sepsis patients (Chow *et al.*, 2005; Vodovotz *et al.*, 2004).

Upon infection, local tissue macrophages begin to secrete pro-inflammatory cytokines that, through activation of the endothelial cells, recruit other phagocytes to the site of infection. Neutrophils, a key phagocyte responder to recruitment, not only directly attack and eliminate microorganisms, but

---

[1] To whom correspondence should be addressed: rparker@pitt.edu; +1-412-624-7364; 1249 Benedum Hall, Pittsburgh, PA 15261 USA

also secret cytokines to amplify the inflammatory response (Murphy *et al.*, 2011). At higher levels of pathogenic challenge, the secretion of pro-inflammatory cytokines in the tissue leads to diffusion into the blood stream; the result is endothelial activation at remote (uninfected) sites, leading to misdirected neutrophil recruitment. In severe sepsis, the neutrophil recruitment to healthy tissues results in tissue damage, the first step toward multi-organ dysfunction (Murphy *et al.*, 2011; Serhan *et al.*, 2010; Kobayashi and DeLeo, 2009). Furthermore, severe challenges lead to low circulating neutrophil concentrations, resulting in the recruitment of young neutrophils into the blood stream (Rodriguez *et al.*, 2009; Orr *et al.*, 2005; Orr *et al.*, 2007). A feedback effect of low circulating neutrophil concentrations is an increase in neutrophil production via the granulocyte-colony stimulating factor (G-CSF) signaling cascade (Tanaka *et al.*, 1996; Navarini *et al.*, 2009).

Low absolute neutrophil count (ANC) in blood is also a limiting factor in some cancer chemotherapy regimens due to drug toxicity (. *e.g.* paclitaxel, docetaxel, vinfluine). The mechanistic effect of chemotherapy on circulating neutrophil count is different in cancer than sepsis. Chemotherapy drug toxicity kills precursor cells (*e.g.*, progenitor cells), causing a drop in circulating ANC (Friberg *et al.*, 2002; Lee and Ratajczak, 2009). Recent studies show that intravenous (I.V.) injection or subcutaneous injection of G-CSF stabilizes the neutrophil concentration in the blood (Nakano and Okutani, 2010; Morstyn *et al.*, 1989). Most models of ANC after chemotherapy are phenomenological (Friberg *et al.*, 2002; de Bock *et al.*, 2009), and though the qualitative characteristics are similar, the dynamics of response are much slower than in sepsis.

Neutrophil dynamics in sepsis and cancer chemotherapy are a complex physiological response. Building from the underlying biology of the neutrophil maturation and G-CSF response cascades, we synthesize a unified model that captures the dynamics of the neutrophil response to inflammatory and chemotherapy challenges. Lipopolysaccharide (LPS) is used as the inflammatory challenge, and docetaxel as the cancer chemotherapeutic.

2. MODELING NEUTROPHIL DYNAMICS

2.1 *Cancer Chemotherapy Model*

The neutrophil model of Friberg *et al.* (2002) was used as the modeling basis (shown as the red blocks in Figure 1). In this model, all cell proliferation from stem cells to immature neutrophils are lumped into the first stage (labeled *Pr* for progenitor cells), and the three following stages (T_1, T_2, and T_3) capture the biological maturation process of neutrophils.

Fig. 1. Neutrophil and G-CSF model block diagram.

Nonlinear feedback (based on the ratio of circulating neutrophil levels to baseline) was used to upregulate neutrophil production in *Pr*. This model employs G-CSF implicitly, though the authors note their feedback structure incorporates the effects of G-CSF among other activators (Friberg *et al.*, 2002). The toxic effect of drug on the progenitor cells is described using an E_{max} model (Friberg *et al.*, 2002), where the progenitor cell elimination term by drug is defined as $\left(\frac{k_{37}}{k_{38}+D(t)}\right)Pr(t)$.

The model developed herein retains the proliferation (*Pr*) and maturation train (T_1, T_2, and T_3) components, as well as the circulating neutrophil pool. However, the feedback regulation of neutrophil proliferation in Figure 1 is explicitly driven by the G-CSF signaling cascade. This increase in biological realism should facilitate the use of the model not only in the case of chemotherapy-induced neutropenia but also to capture the dynamics of other challenges such as immune response or sepsis.

2.2 *LPS Challenge Model*

As an inflammatory challenge, Lipopolysaccharide (LPS) has been used in healthy volunteers to activate the neutrophil response (Suffredini *et al.*, 1995). The LPS challenge is believed to trigger the inflammation cascade through the same mechanisms as those activated in sepsis. Three temporally-spaced dynamic effects are added to the cancer model to capture the effects of LPS on neutrophil response: (i) LPS-induced recruitment of circulating neutrophils (N_c) to tissue; (ii) rapid mobilization of the neutrophil marginal pool (N_p); (iii) recruitment of immature neutrophils (T_1, T_2, and T_3) from bone marrow to the blood stream. In order to capture the sequential effects of LPS on neutrophil recruitment, LPS effects are modeled with two compartments: Equation (1) represents circulating LPS after IV injection, which drives tissue recruitment and the mobilization of neutrophils from the marginal pool; the second LPS state (I_1) (Equation (2)) governs the slower inflammation dynamics that dictate neutrophil recruitment from bone marrow:

$$\frac{dLPS}{dt} = -k_{39}LPS(t) \tag{1}$$

$$\frac{dI_1}{dt} = k_{39}LPS(t) - k_{40}I_1(t) \tag{2}$$

The clearance of LPS (Equation (1)) is integrated in the liver compartment, as shown in Figure 2. The inflammation effect of LPS challenge (Equation (2)) is modeled using a first-order lag. Figure 2 shows the physiological model structure, where the human body is divided into 16 compartments representing important tissues for inflammation. Compartments are connected via the circulation of blood and the heart/lung compartment. Each tissue contains a vascular and extravascular subcompartment. A detailed model of inflammation dynamics in the tissue extravascular space was constructed for pathogen/ phagocyte/IL-1 interactions; space constraints preclude the full description of this model here.
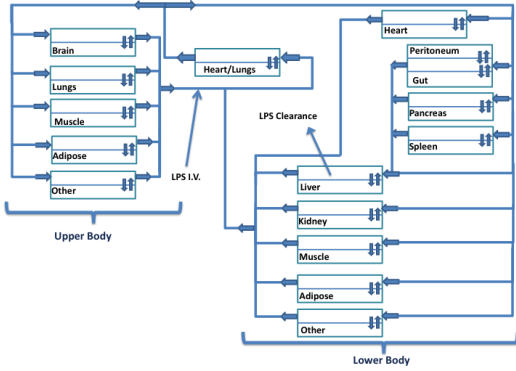
Fig. 2. Physiological model of inflammation.

2.3 Biological Feedback on Neutrophil Production

The G-CSF-neutrophil signaling cascade has been identified (Serhan *et al.*, 2010; Stark *et al.*, 2005), as shown in Figure 1. The neutrophil concentration (N_c) in the blood down-regulates the production of IL-23 through N_d, the amount of neutrophils undergoing apoptosis; decreases in N_d promote IL-23 production. This IL-23 activation upregulates the production of IL-17 through the activation of T cells. The increase in IL-17 concentration leads to the activation of stomal cells, which increases circulating G-CSF levels. Finally, the G-CSF signal induces the production of progenitor cells (Stark *et al.*, 2005).

2.4 The Neutrophil Model

$$\frac{dPr}{dt} = \left(k_{41} + \frac{k_{32}GCSF(t)}{k_{33}+GCSF(t)}\right)S - k_{tr}Pr(t)$$
$$ - \left(\frac{k_{37}}{k_{38}+D(t)}\right)Pr(t) \tag{3}$$

$$\frac{dT_1}{dt} = k_{tr}Pr(t) - k_{tr}\left(1+1.5\frac{I_1(t)}{k_{36}+I_1(t)}\right.$$

$$\left. +1.5\frac{IL1(t)}{k_{36}+IL1(t)}\right)T_1(t) \tag{4}$$

$$\frac{dT_2}{dt} = k_{tr}T_1(t) - k_{tr}\left(1+1.5\frac{I_1(t)}{k_{36}+I_1(t)}\right.$$

$$\left. +1.5\frac{IL1(t)}{k_{36}+IL1(t)}\right)T_2(t) \tag{5}$$

$$\frac{dT_3}{dt} = k_{tr}T_2(t) - k_{tr}\left(1+1.5\frac{I_1(t)}{k_{36}+I_1(t)}\right.$$

$$\left. +1.5\frac{IL1(t)}{k_{36}+IL1(t)}\right)T_3(t) \tag{6}$$

$$\frac{dN_c}{dt} = k_{tr}T_3(t) - Tissue + 1.5k_{tr}\left(\frac{I_1(t)}{k_{36}+I_1(t)} + \frac{IL1(t)}{k_{36}+IL1(t)}\right)$$

$$(T_1(t)+T_2(t)+T_3(t)) - k_{tr}\left(1-\frac{IL1(t)}{k_{36}+IL1(t)}\right)N_c(t)$$

$$+k_{tr}\left(1+10\frac{IL1(t)}{k_{36}+IL1(t)}\right.$$

$$\left. +k_{34}\frac{GCSF(t)}{k_{35}+GCSF(t)}\right)N_p(t) \tag{7}$$

$$\frac{dN_p}{dt} = k_{tr}\left(1-\frac{IL1(t)}{k_{36}+IL1(t)}\right)N_c(t) - k_{tr}\left(1+10\frac{IL1(t)}{k_{36}+IL1(t)}\right.$$

$$\left. +k_{34}\frac{GCSF(t)}{k_{35}+GCSF(t)}\right)N_p(t) \tag{8}$$

$$\frac{dN_d}{dt} = \frac{k_5N_c(t)}{k_8+N_c(t)}\left(1-\frac{k_6GCSF(t)}{k_7+GCSFt}\right) - k_9N_d(t) \tag{9}$$

$$\frac{dIL23}{dt} = \left(k_{10} - \frac{k_{11}N_d(t)}{k_7+N_d(t)}\right)N_d(t) - k_{12}IL23(t) \tag{10}$$

$$\frac{dT_a}{dt} = \left(k_{15} + \frac{k_{16}IL23(t)^2}{k_{17}^2+IL23(t)^2}\right)T_i(t) - \frac{k_{13}k_{14}^2}{k_{14}^2+T_a^2}T_a(t) \tag{11}$$

$$\frac{dT_i}{dt} = \frac{k_{13}k_{14}^2}{k_{14}^2+T_a^2}T_a(t) - \left(k_{15} + \frac{k_{16}IL23(t)^2}{k_{17}^2+IL23(t)^2}\right)T_i(t) \tag{12}$$

$$\frac{dIL17}{dt} = k_{18}T_a(t) - k_{19}IL17(t) \tag{13}$$

$$\frac{dS_c}{dt} = \frac{k_{20}}{k_{21}+IL17(t)}IL17(t) - \frac{k_{22}k_{23}}{k_{23}+S_c(t)}S_c(t) \tag{14}$$

$$\frac{dGCSF}{dt} = \frac{k_{24}S_c(t)^2}{k_{25}^2+S_c(t)^2}S_c(t) - \left(k_{26} + \frac{k_{27}N_c(t)}{k_{28}+N_c(t)}\right)GCSF(t)$$

$$+k_{29}GCSF_T(t) - k_{30}GCSF(t) \tag{15}$$

$$\frac{dGCSF_T}{dt} = k_{30}GCSF(t) - k_{29}GCSF_T(t) - k_{31}GCSF_T(t) \tag{16}$$

Equations (3)-(8) describe the neutrophil dynamics from the progenitor cells to circulating neutrophils, including the marginal pool. Recruitment of immature neutrophils from Equations (4)-(6) to the blood stream in response to an LPS challenge follows Michaelis-Menten kinetics driven by both the LPS effect Equation (2) and the G-CSF effect. Progenitor cell proliferation in Equation (3), and the induction of neutrophil death in Equation (9), are modeled using the dynamics in (Shochat *et al.*, 2007). The circulating neutrophil (N_c) equation has a tissue uptake term, driven by the extravascular inflammation response in the physiological model. The G-CSF-induced regulation of neutrophil proliferation is governed by Equations (9)-(15). The production of IL-23 and IL-17, and the activation of T cells (T_a) and stromal cells (S_c), are described as second-order Hill functions to capture the response of the G-CSF signaling cascade (slow initial response, increasing nonlinearly with increasing signal). For G-CSF, production is a saturating function of the number of activated stromal cells, while degradation was modeled using first order

Table 1. Neutrophil model parameters(P).

P	Value	Unit	P	Value	Unit
k_1	0.006	$\frac{pg}{ml}$	k_{21}	$5*10^4$	$\frac{pg}{ml}$
k_2	14.5511	—	k_{22}	0.0188	$\frac{1}{min}$
k_3	$1.56*10^{-8}$	$\frac{pg}{ml}$	k_{23}	$3.2*10^4$	$\frac{cell}{min}$
k_4	8000	$\frac{pg}{ml}$	k_{24}	0.0085	$\frac{pg}{cell.ml}$
k_5	0.0016	$\frac{1}{min}$	k_{25}	$2.5*10^3$	$\frac{cell}{min}$
k_6	0.25	—	k_{26}	0.001	$\frac{1}{min}$
k_7	10^5	$\frac{pg}{ml}$	k_{27}	0.0066	$\frac{1}{min}$
k_8	10^7	$\frac{cell}{min}$	k_{28}	10^7	$\frac{cell}{min}$
k_9	0.0858	$\frac{1}{min}$	k_{29}	0.004	$\frac{1}{min}$
k_{10}	0.11843	$\frac{1}{min}$	k_{30}	$9*10^{-11}$	$\frac{1}{min}$
k_{11}	0.1184	$\frac{1}{min}$	k_{31}	0.00073	$\frac{1}{min}$
k_{12}	0.0253	$\frac{1}{min}$	k_{32}	0.00159	$\frac{1}{min}$
k_{13}	0.3603	$\frac{1}{min}$	k_{33}	$6*10^4$	$\frac{pg}{ml}$
k_{14}	10^6	$\frac{cell}{min}$	k_{34}	8.4170	—
k_{15}	$8.48*10^{-7}$	$\frac{1}{min}$	k_{35}	10^4	$\frac{pg}{ml}$
k_{16}	24.9738	$\frac{1}{min}$	k_{36}	$3.5*10^9$	$\frac{pg}{ml}$
k_{17}	50000	$\frac{pg}{ml}$	k_{37}	77.5	$\frac{pg}{ml}$
k_{18}	0.0062	$\frac{pg}{cell.ml}$	k_{38}	0.0016	$\frac{pg}{ml}$
k_{19}	0.0922	$\frac{pg}{ml}$	k_{39}	0.00045	$\frac{1}{min}$
k_{20}	0.002	$\frac{pg}{cell.ml}$	k_{40}	0.0091	$\frac{1}{min}$
–	–	–	k_{41}	0.000035	$\frac{pg}{ml}$

Fig. 3. Published (mean ± std. dev.) and model fit to data of neutrophil and G-CSF concentration in response to LPS challenge (Suffredini *et al.*, 1995).

Fig. 4. Dynamics of different neutrophil states and LPS.

kinetics and an effective clearance rate dependent on the concentration of circulating neutrophils. Tissue G-CSF, used for subcutaneous injection, exchanges with blood G-CSF according to the concentration gradient and has a first order degradation rate. Model parameters are shown in Table 1, and initial conditions are: $N_c = 5 \times 10^6$ cells/ml; $GCSF = 18$ pg/ml; and neutrophil half-life ≈ 6 hr (Murphy *et al.*, 2011; Serhan *et al.*, 2010). For all simulations performed, the parameter values were held constant. The parameters k_{15}, k_{17}, k_{31}, k_{34}, and k_{40} were estimated using nonlinear least-squares (Hoggs *et al.*, 2010) (*lsqnonlin* function in MATLAB, the MathWorks, Natick, MA) in order to minimize the sum of squared error between the model and LPS experimental data (see below). Other parameters were taken from the literature.

3. RESULTS

3.1 *Human LPS Challenge*

To study the neutrophil dynamics in the human body under the influence of inflammation, Suffredini *et al.* (1995) conducted a study in which endotoxin from Escherichia coli was administered i.v. (4 ng/kg of body weight, 6 human subjects) over 1 min. Serial blood samples measured plasma neutrophils, G-CSF levels, and other inflammation-associated cytokines and chemokines. Experimental data and simulation results are shown in Figure 3. Although the model underpredicted the neutrophil concentration at early time points, the observed neutrophil dynamics were captured well beyond 5 hours. (Figure 3a). Some discrepancy is observed between the G-CSF experimental data and the simulation results (Figure 3b) in terms of peak timing, though the large error bars from the measurement data – likely a result of interpatient variability – reduce the confidence in the mean value of the 3 and 6 hr time points. On
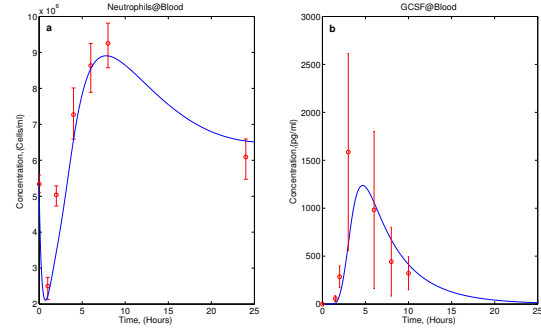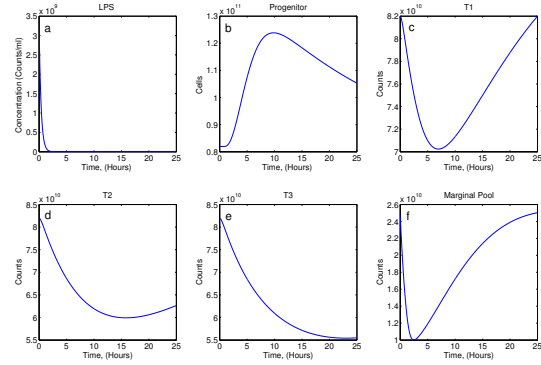
the whole, the G-CSF model follows the experimental data.

The simulation results also provide insight into the complicated dynamics of the physiological inflammatory response, especially neutrophil production and recruitment dynamics. Figure 4 shows simulated LPS levels in the blood as well as different neutrophil compartments. Although the LPS concentration is almost zero after 3 hours (Figure 4a), the effects of the LPS challenge on neutrophil production and recruitment continue for more than 10 hours (Figure 4b, c, d, and e). The most mature neutrophils compartment (T3, Figure 4e) drops more than 30% of its steady value, while the neutrophil levels of T2 and T1 (Figures 4d and 4e) drop about 23% and 10%, respectively. As a result of the initial decrease in circulating neutrophils, progenitor cell production yields a 50% increase in the number of cells in the *Pr* compartment (Figure 4b). Also driven by the rapid initial neutrophil redistribution to tissues, the marginal pool neutrophil count drops to about 60% of its steady state value after 3 hours; at this point the circulating neutrophil count returns to its steady state value, and the marginal pool begins to recover slowly toward its steady level.
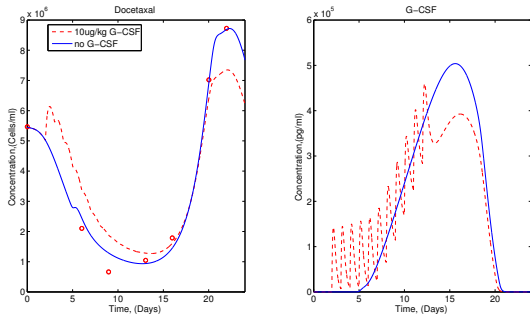
Fig. 5. Data (Friberg *et al.*, 2002) and model fit of ANC after 1 hr docetaxel infusion at 100 mg/m^2 (blue solid), and G-CSF subcutaneous injection at 10ug/kg/day from days 2 to 12 (red dashed)

3.2 *Cancer Model*

To study the effects of chemotherapy treatment on ANC, Friberg *et al.* (2002) investigated response to a variety of drugs that induce myelosuppresion. We simulated a pharmocokinetic model of docetaxel built in our lab (a physiologically-structured model that provides circulating docetaxel predictions equivalent to experimentally-validated 3-compartment models) and compared the neutrophil model predictions to the docetaxel response data from (Friberg *et al.*, 2002) patients receiving 1 hr infusion of docetaxel at 100 mg/m^2). The simulation and experimental results are shown in Figure 5. Using the parameters in Table 1, the model matches the experimental data, except for an overprediction of ANC at day 8. As expected, G-CSF injection during chemotherapy maintained higher ANC concentration from days 2 to 12, reducing the depth of nadir – a key driver of treatment schedule changes for cancer chemotherapy patients. With the ability to capture both fast neutrophils dynamics (LPS challenge) and slow neutrophil dynamics (chemotherapy), a suitable test is an intermediate speed challenge in the form of cecal ligation and puncture (CLP) – a common preclinical model of inflammation and sepsis.

3.3 *CLP Challenge*

The advantage of CLP challenge over LPS challenge is that the inflammation response initiated by infection in a local tissue will migrate to other tissue (spillover effects), just like in experimental and clinical sepsis. CLP involves the puncture of the cecum of the large intestine using a fine-guage needle, leading to the release of intestinal bacteria into the peritoneal cavity. Initial bacterial load establishes the severity of the CLP challenge. Simulation results are shown in Figure 6. Following a moderate challenge (10^6 cells/ml), circulating neutrophils initially decrease because of recruitment to the site of infection, a result of IL-1 induced endothelial activation. The clearance of pathogen out of the peritoneum leads to the end of recruitment of neutrophils to the infection
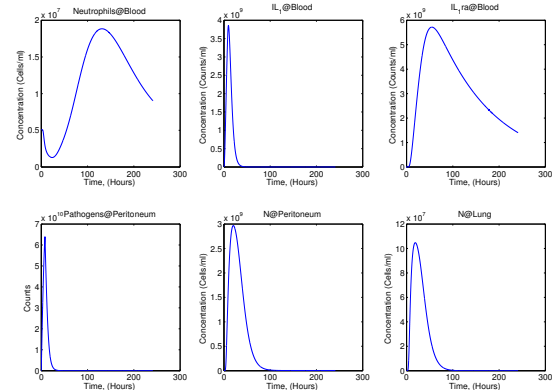

Fig. 6. Inflammation dynamics after a moderate CLP challenge

site. Following this, IL-1, and its anti-inflammatory complement IL-1ra, are cleared from the blood stream through liver and kidney clearance. To help offset the initial decrease in circulating neutrophils, G-CSF-induced feedback leads to production in *Pr* and a more rapid recovery of circulating neutrophil count (including overshoot of baseline).

Inflammatory challenges also lead to tissue damage, often through the recruitment of neutrophils to uninfected sites. Once activated, these neutrophils damage otherwise healthy tissues. The simulation also suggests that the neutrophils are misdirected from the site of infection to healthy tissue due to the systemic activation of endothelium by circulating IL-1. The result, as shown in Figure 6, is an increase in the neutrophil count in the lung. This is an undesirable side-effect of systemic inflammation, and is considered the first step along the path to multiple organ dysfunction (Murphy *et al.*, 2011). Moreover, the G-CSF concentration reaches its maximum level about 30,000 pg/ml (not shown), which agrees with the reported G-CSF concentration in patients with sepsis (Tanaka *et al.*, 1996; Cebon *et al.*, 1994). Overall, the simulation results capture critical dynamics of the CLP challenge, and give a certain level of confidence in using the model as the framework to test the effect of sepsis treatments on neutrophil dynamics.

4. SUMMARY AND DISCUSSION

A neutrophil dynamics model based on the biology of neutrophils production through the G-CSF signaling cascade was developed. The model was calibrated to an inflammatory LPS challenge for both neutrophil and G-CSF dynamics. The model was then tested with the slower dynamics of chemotherapy challenge, and it accurately predicted neutrophil dynamics following IV docetaxel administration. Finally, the model was used to study neutrophil dynamics after CLP. From the simulation results, the G-CSF concentration in CLP captured the maximum range reported in

the literature. This model of neutrophil dynamics, including the biologically-derived feedback of G-CSF on cell proliferation, provides a more detailed view of neutrophil dynamics in response to multiple disparate challenges. Furthermore, its ability to fit these challenges makes it a candidate to contribute to treatment design for sepsis and cancer chemotherapy, where neutrophils play a significant role in limiting treatment (cancer) or response (inflammation/sepsis).

5. ACKNOWLEDGMENTS

6. REFERENCES

Angus, D. C. and R.S. Wax (2001). Epidemiology of sepsis: An update. *Critical Care Medicine* **29**(7), S109–S116.

Cebon, J., J. E. Layton, D. Maher and G. Morstyn (1994). Endogenous haemopoietic growth factors in neutropenia and infection. *British Journal of Haematology* **86**(2), 265–274.

Chow, C. C., G. Clermont, R. Kumar, C. Lagoa, Z. Tawadrous, D. Gallo, B. Betten, J. Bartels, G. Constantine, M.P. Fink, T.R. Billiar and Y. Vodovotz (2005). The acute inflammatory response in diverse shock states. *Shock* **24**, 74–84.

de Bock, G., H. Putter, J. Bonnema, J. van der Hage, H. Bartelink and C. van de Velde (2009). The impact of loco-regional recurrences on metastatic progression in early-stage breast cancer: a multistate model. *Breast Cancer Research and Treatment* **117**, 401–408.

Friberg, L. E., A. Henningsson, H. Maas, L. Nguyen and M. O. Karlsson (2002). Model of chemotherapy-induced myelosuppression with parameter consistency across drugs. *Journal of Clinical Oncology* **20**(24), 4713–4721.

Hoggs, J.S., G. Clermont and R.S. Parker (2010). Acute inflammation treatment via particle filter state estimation and mpc. In: *Proceedings of the 9th International Symposium on Dynamics and Control Process Systems*. Lueven,Belgium. pp. 258–263.

Kobayashi, S. D. and F. R. DeLeo (2009). Role of neutrophils in innate immunity: a systems biology-level approach. *Wiley Interdisciplinary Reviews: Systems Biology and Medicine* **1**(3), 309–333.

Lee, H. and M. Ratajczak (2009). Innate immunity: a key player in the mobilization of hematopoietic stem/progenitor cells. *Archivum Immunologiae et Therapiae Experimentalis* **57**, 269–278.

Mathe, J.L., A. Ledeczi, A. Nadas, J. Sztipanovits, J.B. Martin, L.M. Weavind, A. Miller, P. Miller and D.J. Maron (2009). A model-integrated, guideline-driven, clinical decision-support system. *Software, IEEE* **26**(4), 54 –61.

Morstyn, G., L. Campbell, G. Lieschke, J. E. Layton, D. Maher, M. O'Connor, M. Green, W. Sheridan, M. Vincent and K. Alton (1989). Treatment of chemotherapy-induced neutropenia by subcutaneously administered granulocyte colony-stimulating factor with optimization of dose and duration of therapy. *Journal of Clinical Oncology* **7**(10), 1554–1562.

Murphy, K., P. Travers and M. Walport (2011). *Janeway's Immunobiology*. Taylor and Francis.

Nakano, Y. and R. Okutani (2010). Perioperative management for a patient with chronic pancytopenia: a case of aplastic anemia with persistent neutropenia following preoperative administration of g-csf. *Journal of Anesthesia* **24**, 268–271.

Navarini, A. A., K. S. Lang, A. Verschoor, Mi. Recher, A. S. Zinkernagel, V. Nizet, B. Odermatt, H. Hengartner and R.M. Zinkernagel (2009). Innate immune-induced depletion of bone marrow neutrophils aggravates systemic bacterial infections. *Proceedings of the National Academy of Sciences* **106**(17), 7107–7112.

Orr, Y., D. P. Wilson, J. M. Taylor, P. G. Bannon, C. Geczy, M. P. Davenport and L. Kritharides (2007). A kinetic model of bone marrow neutrophil production that characterizes late phenotypic maturation. *American Journal of Physiology - Regulatory, Integrative and Comparative Physiology* **292**(4), R1707–R1716.

Orr, Y., J. M. Taylor, P. G. Bannon, C. Geczy and L. Kritharides (2005). Circulating cd10+cd16low neutrophils provide a quantitative index of active bone marrow neutrophil release. *British Journal of Haematology* **131**(4), 508–519.

Parker, R. S. and G. Clermont (2010). Systems engineering medicine: engineering the inflammation response to infectious and traumatic challenges. *Journal of The Royal Society Interface* **7**(48), 989–1013.

Rivers, E., B. Nguyen, S. Havstad, J. Ressler, A. Muzzin, B. Knoblich, E. Peterson and M. Tomlanovich (2001). Early goal-directed therapy in the treatment of severe sepsis and septic shock. *New England Journal of Medicine* **345**(19), 1368–1377.

Rodriguez, S., A. Chora, B. Goumnerov, C. Mumaw, W. S. Goebel, L. Fernandez, H. Baydoun, H. HogenEsch, D. M. Dombkowski, C. A. Karlewicz, S. Rice, L. G. Rahme and N. Carlesso (2009). Dysfunctional expansion of hematopoietic stem cells and block of myeloid differentiation in lethal sepsis. *Blood* **114**(19), 4064–4076.

Rosinski, M., M. L. Yarmush and F. Berthiaume (2004). Quantitative dynamics of in vivo bone marrow neutrophil production and egress in response to injury and infection. *Annals of Biomedical Engineering* **32**, 1109–1120.

Serhan, C.N., P.A. Ward and D.W. Gilroy (2010). *Fundamentals of Inflammation*. Cambridge University Press.

Shochat, E., V. Rom-Kedar and L. Segel (2007). G-csf control of neutrophils dynamics in the blood. *Bulletin of Mathematical Biology* **69**, 2299–2338.

Stark, M.A., Y. Huo, T. L. Burcin, M. A. Morris, T. S. Olson and K. Ley (2005). Phagocytosis of apoptotic neutrophils regulates granulopoiesis via il-23 and il-17. *Immunity* **22**(3), 285 – 294.

Suffredini, A. F., D. Reda, S. M. Banks, M. Tropea, J. M. Agosti and R. Miller (1995). Effects of recombinant dimeric tnf receptor on human inflammatory responses following intravenous endotoxin administration. *The Journal of Immunology* **155**(10), 5038–5045.

Summers, C., S. M. Rankin, A.M. Condliffe, N. Singh, A. M. Peters and E. R. Chilvers (2010). Neutrophil kinetics in health and disease. *Trends in Immunology* **31**(8), 318 – 324.

Tanaka, H., K. Ishikawa, M. Nishino, T. Shimazu and T. Yoshioka (1996). Changes in granulocyte colony-stimulating factor concentration in patients with trauma and sepsis. *The Journal of Trauma* **40**(5), 718–726.

Vodovotz, Y., G. Clermont, C. Chow and G. An (2004). Mathematical models of the acute inflammatory response.. *Current Opinion in Critical Care* **10**(5), 383–390.